A Frustrated Antiferromagnetic Ising Model

Shadab Ahamed

Undergraduate Programme
Indian Institute of Science, Bangalore

Under the Mentorship of

R. Ganesh

The Institute of Mathematical Sciences, Chennai

Acknowledgement

I would express sincere gratitude to my mentor Dr. R. Ganesh, who guided me through the project and introduced me to several exciting realms of Statistical Physics. It would have been impossible to complete this project without his encouragement at every stage. I am also grateful to Dr. Bimla Danu, who proved to be a constant source of support and advice, and helped me in the hour of need. I would thank my fellow summer interns too, who made my stay at Chennai a memorable one. Lastly, I would also thank The Institute of Mathematical Sciences, Chennai for providing me with this oppotunity to do a project.

Contents

1 Overview

In materials that exhibit Antiferromagnetism, the atomic or molecular dipoles (usually related to the spins of electrons) align in a regular manner, with the neighbouring spins (on different sublattices) pointing in opposite directions. Generally, the antiferromagnetic order is known to exist at sufficiently low temperatures, but vanishes at higher temperatures due to thermal agitation of the lattice and becomes paramagnetic [2]. The temperature at and above which this transition occurs is known as the Néel temperature (named after Louis Néel, who first identified this type of magnetic ordering). Unlike ferro-magnetism, antiferromagnetism can give rise to multiple ground states in two-dimensional lattices, due to the phenomenon of frustration; inability to attain a single ground state due to certain geometry of the lattices. In this project,we have performed the classical Monte Carlo (MC) simulation on a two-dimensional $J' - J$ Ising lattice using Importance sampling, in order to produce some useful thermodynamic averages, like $\langle E\rangle, \langle E^2\rangle, \langle M\rangle, \langle |M|\rangle, \langle M^2\rangle$, etc. as a function of temperature, in a certain temperaure range. Later, we have varied the value of J'/J (certain parameter of the lattice) from 0.0 through 1.0, and tried to observe how the Critical Temperature changes as a function of J'/J. We have also plotted the histograms of the number of squares assuming a particular configuration, and exploited this idea to locate T_c and T_s.

2 $J' - J$ Ising Model

The classical Ising Model, named after the physicist Ernst Ising, is a Mathematical model to explain magnetic behaviour in Statistical Mechanics. It consists of discrete variables representing the magnetic dipole moments of individual atomic spins, that could assume one of the values from set $\{-1, +1\}$. These spins are arranged in a lattice. Apparently, the two-dimensional square-lattice Ising model is one of the simplest Mathematical models to show a phase transition [5].

2.1 Lattice Geometry

Consider a two-dimensional square lattice of side L, with N lattice points, where $N = L \times L$. We will assume periodic boundary conditions all the time. A spin on any lattice site can be either "up", i.e. +1 or "down", i.e. -1. A spin on site i of the lattice is denoted by σ_i. Each spin can interact with its nearest neighbours with a coupling constant J and with its nearest neighbours along the main-diagonal of each small square with a coupling constant of J' (Figure 1). The coupling constants represent the interactions between spins. Henceforth, we will refer to these interactions as *bonds*. The energy, E of the lattice is thus given by

$$E = J \sum_{<i,j>} \sigma_i \sigma_j + J' \sum_{[i,j]} \sigma_i \sigma_j \tag{1}$$

where $< i, j >$ represents the nearest neighbours,
$[i, j]$ represents the diagonal neighbours.

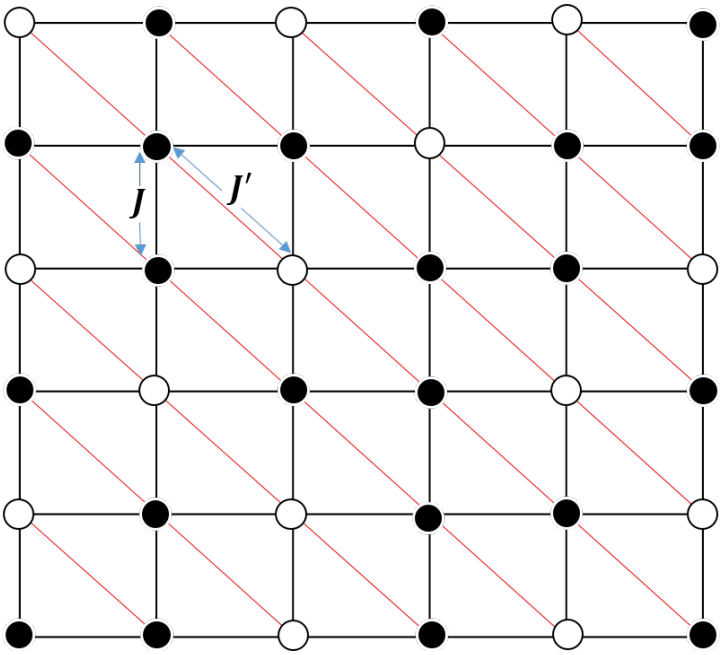

Figure 1: A randomly generated Ising Lattice, with red bonds representing the J' interactions and black bonds representing the J interactions. The black "dots" stand for the "up" or (+) spins and the white ones for the "down" or (-) spins

2.2 Ground States as a function of J'/J

We have fixed the value of $J = 1$, and varied the value of J' from 0.0 through 1.0. We expect the following to happen:

(i) For $J' = 0$, interactions between the diagonal spins vanish and we get a square lattice, where the interations exist between neighbouring spins along the horizontal and vertical directions only . Since $J > 0$, the nearest neighbours will want to align oppositely in order to minimize energy E, that is, if one is $+1$, the other will be -1 and vice-versa. If any particular bond consists of spins that are oppositely aligned, then it is considered to be a *happy* bond, if it has spins aligned in the same direction, then it is considered to be an *unhappy* bond. Each small square can be in one of the $2^4 = 16$ configurations (Figure 2), the system will choose one of the two configurations in which all (or atleast a maximum number of) the bonds are *happy* in order to attain minimum energy. Hence, for $J' = 0$, two ground states are possible as shown in Figure 3 (a) and (b).

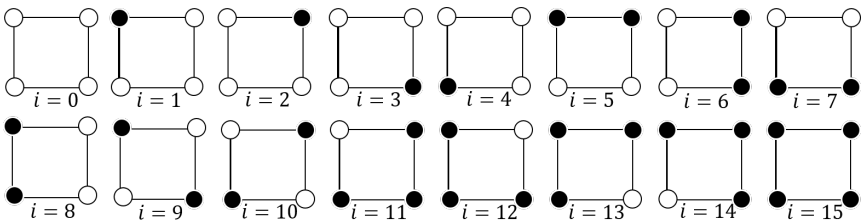

Figure 2: All the possible $2^4 = 16$ configurations (numbered from $i = 0$ to $i = 15$) for a square

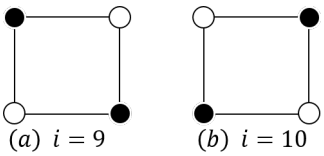

Figure 3: The two possible ground states for a square that ensure minimum energy

(ii) For $J' > 0$ but not very close to 1.0, the J' bonds are still weaker than the J bonds ($J'/J < 1$), and hence, the squares will have an *unhappy* bond along J' and a *happy* one along J . As a result, the system will behave similar to the case of a perfectly square lattice ($J' = 0$).

(iii) For J' very close to but lesser than 1, the J' bonds will have alomst equal interaction strength as compared to the J bonds, and hence we expect to see some patches on the lattice with slight deviation from the previous case, since now, an *unhappy* bond can even lie along J, due to the small energy difference between J' and J.

(iv) For $J' = 1$, the diagonal bonds become equal in interaction to the horizontal and vertical bonds. On a closer look at the system, we find that it is topologically similar to a two-dimensional Triangular lattice (Figure 4). Unlike in the case of a square, it is impossible for a triangle to have all the three bonds along its three sides *happy* (geometric frustration) (Figure 5). There are only two possiblities, viz, either all the three bonds are *unhappy* or two bonds are *happy* and one *unhappy*, the latter being the configuration pertaining to minimum energy. Hence, the system will choose the spins in a way such that all the triangles have two *unhappy* and one *happy* bond. As a result, now the system can access multiple ground states at low enough temperatures as well.

(v) For $1 < J' < 2$, the J' bonds become stonger than the J bonds, and hence it would be more likely that a *happy* bond will lie along J' and since each triangle must have two *happy* bonds, one of the J will be *happy* and another *unhappy*. In this case too, the system can have multiple ground states.

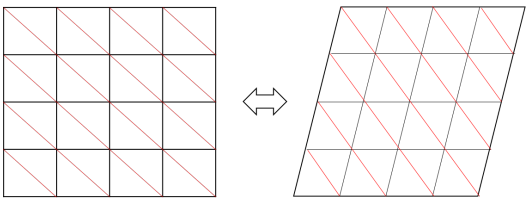

Figure 4: Sketch showing square and triangular lattices

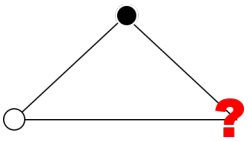

Figure 5: Geometric frustration on a triangle

3 The Metropolis-Hastings Algorithm

In statistics, the Metropolis-Hastings Algorithm is a Markov Chain Monte Carlo (MCMC) technique for drawing a sequence of random samples from a probabil-

ity distribution for which direct sampling might be difficult. Thus, Monte Carlo technique can be efficiently used in the simulation of systems in which stochastic processes occur [4]. We have successfully used this technique to solve for thermodynamic *observables* of the Ising model.

We have used a simple single-flip algorithm in order to simulate the Ising lattice. The implementation was carried out using a C++ code. The way the Metropolis algorithm was implemented can be described using the following procedure [3]:

(1) Randomly generate a lattice.

(2) Choose a site i on the lattice randomly.

(3) Calculate the ΔE that results when the spin at the site i is flipped.

(4) Check whether ΔE is positive, negative or zero.

(5) (i) if $\Delta E < 0$, flip the spin.

(ii) if $\Delta E \geq 0$, flip the spin with probability $e^{\frac{-\Delta E}{k_B T}}$.

(6) Go to (2) and repeat the process several times.

After allowing the system to settle down to equilibrium following 5000 Monte Carlo steps, we have calculated the sample mean of the thermodynamic *observables* over another 100000 Monte Carlo steps for each value of temperature in a specific range (usually $T = 0.1\frac{J}{k_B}$ to $T = 5.0\frac{J}{k_B}$) .

4 Calculation of *observables*

The *observables* of interest $\langle E\rangle, \langle E^2\rangle, \langle M\rangle, \langle |M|\rangle, \langle M^2\rangle$, etc. were calculated in the following way:

$$\langle A\rangle = \frac{1}{N}\sum_{\alpha}^{N} A(\alpha) \tag{2}$$

where $\langle A\rangle$ could be $\langle E\rangle, \langle E^2\rangle, \langle M\rangle, \langle |M|\rangle, \langle M^2\rangle$, etc. Magnetisation, M, for a square lattice antiferromagnetic system, which is also the *order parameter* in this case, is defined as:

$$M = \sum_{i=1}^{N} (-1)^i \sigma_i \tag{3}$$

At the Néel transition temperature, we expect a marked fluctuation in these quantities. To illustrate this fluctuation, we would use the variance of the random variable, $(\Delta A)^2 = \langle A^2\rangle - \langle A\rangle^2$. This leads us to the idea of calculating the specific heat capacity, C_v and magnetic susceptibility, χ_T, given by the following equations,

$$C_v = \frac{\partial E}{\partial T} = \frac{(\Delta E)^2}{k_B T} = \frac{\langle E^2\rangle - \langle E\rangle^2}{k_B T^2} \tag{4}$$

$$\chi_T = \frac{\partial M}{\partial T} = \frac{(\Delta M)^2}{k_B T} = \frac{\langle M^2 \rangle - \langle M \rangle^2}{k_B T} \tag{5}$$

A fourth-order Binder's Cumulant was calculated, which was eventually used to locate the Néel temperature.

$$U_L = 1 - \frac{\langle M^4 \rangle_L}{3\langle M^2 \rangle_L^2} \tag{6}$$

Entropy per spin, $s(T)$ was evaluated at each temperature, T using the following equation [6],

$$s(T) = s(\infty) - \int_T^\infty \frac{c_v(\tau)}{\tau} d\tau \tag{7}$$

where $c_v(\tau)$ is the specific heat per spin at temperature τ. Since the lattice is randomized, at large temperatures each of the N spins can be either $+1$ or -1 with equal probabilities. Hence, the total number of microstates Ω of the system will be $\Omega = 2^N$. Therefore, the specific entropy will be given by, $s = \frac{S}{N} = \frac{k_B ln(2^N)}{N} = k_B ln(2)$. Also, since in our simulation, the temperature scale is discrete, the integral in Equation (7) changes to a summation. $d\tau$ was equal to 0.1 $\frac{J}{k_B}$, since we varied the temperature in steps on 0.1 $\frac{J}{k_B}$. $T = \infty$ was assumed to be that finite temperature, T_f after which the value of c_v practically turned zero, i.e., of the order of $10^{-5} \frac{J}{k_B^2}$. Hence, we have the following formula for $s(T)$,

$$\implies s(T) = ln(2) - \sum_{\tau=T}^{T_f} \frac{c_v}{\tau} d\tau \tag{8}$$

Each square on the lattice can be assigned a configuration number from 0 to 15, based on Figure 2. For the square limit ($J' = 0$), we have plotted a histogram of number of different configurations for a given temperature, T. Similarly, for the triangular limit ($J' = 1$), one can count the number of triangles with one *unhappy* bond and those with three *unhappy* bonds, and appropriate histograms can be plotted in this case too. A careful assessment of these histograms at various temperatures might help us locate the Critical Temperature.

5 The Square Limit ($J'/J = 0$)

The C++ code was run for different values of L and various curves were plotted. The results have been discussed below. The temperature has been varied in steps of 0.1 $\frac{J}{k_B}$ in all cases, expect while plotting Binder's Cumulant vs temperature, where it has been varied in steps of 0.01 $\frac{J}{k_B}$, for better accuracy while locating the Critical Temperature.

5.1 Energy and Specific Heat

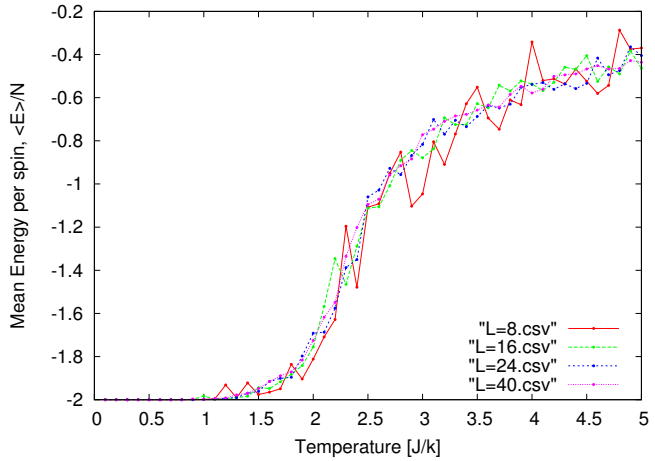

Figure 6: Mean Energy per spin, $\langle E \rangle / N$ vs Temperature, T

In Figure 6, Mean Energy per spin as a function of temperature has been plotted for different lattice sizes. The steep rise in the curves point towards a possible phase transition. One can see that for smaller lattice sizes, the fluctuation in the curve is more. At higher temperatures, due to randomness, the lattice has a relatively higher energy, whereas for lower temperatures, we find that the system stabilizes to $E/N = -2J$ as expected.

In Figure 7, the Specific Heat per spin as a function of temperature is given. In order to mark the Critical Temperature, we need to look for divergence in the curve. Clearly, we do not see any divergence, but there exists a progressive steepening of the curve with increasing lattice sizes.

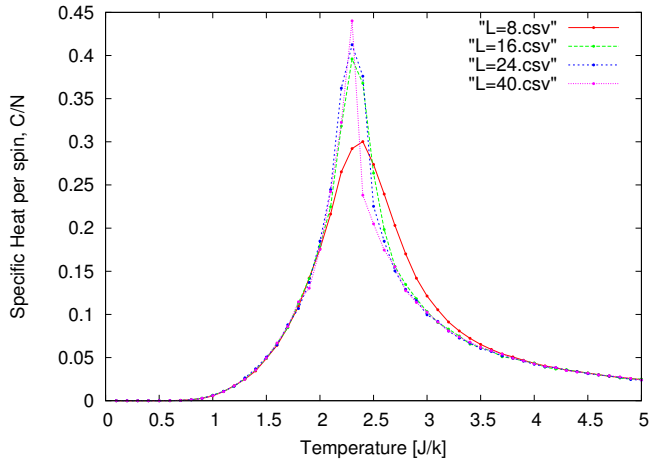

Figure 7: Specific Heat per spin, C/N vs Temperature, T

The point of maxima may or may not be the point of divergence, depending upon whether the Critical Temperature exists or not.

5.2 Magnetization and Susceptibility

Figure 8 shows the plot of Mean Magnetization per spin as a function of temperature for various lattice sizes. As expected, at lower temperatures, the system could assume one of the two possible states (one with $M = -1$ and the other with $M = +1$). At higher temperatures, the system becomes random and has no overall magnetization.

Figure 9 has been plotted to show how the Mean Absolute Magentization per spin varies as a function of temperature. The sharp decrease in the curve becomes more and more prominent with increasing lattice size, signalling towards the possibility of a phase transition.

Figure 10 shows the variation of Magnetic Susceptibility per spin as a function of temperature for various lattice sizes. The peaks of these curves seem to soar higher with increasing lattice size. Again, we expected a divergence near the critical point, which is not visible in the graph due to the small sizes of the lattices used during simulations.

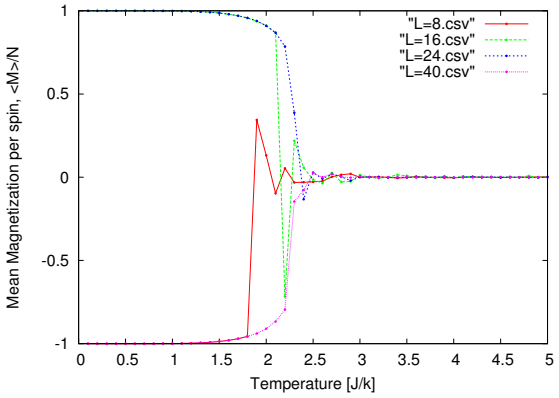

Figure 8: Mean Magnetization per spin, $\langle M \rangle / N$ vs Temperature, T

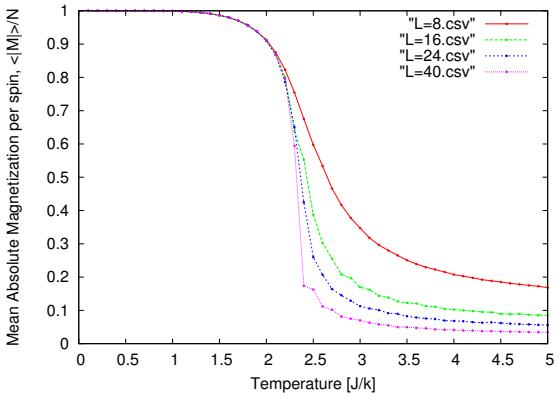

Figure 9: Mean Absolute Magnetization per spin, $\langle |M| \rangle / N$ vs Temperature, T

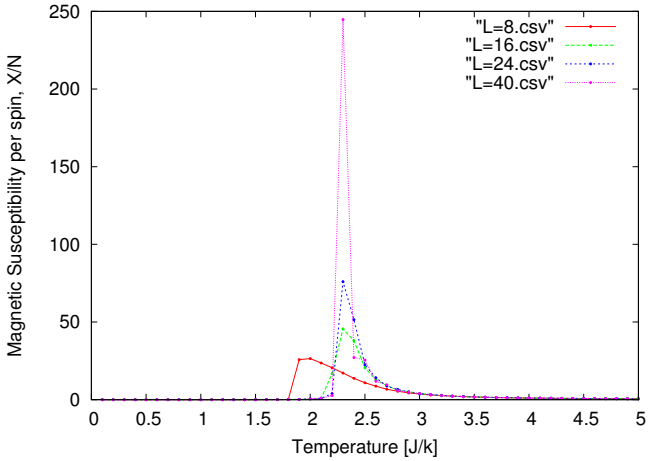

Figure 10: Magnetic Susceptibility per spin, χ_T / N vs Temperature, T

5.3 Binder's Cumulant and Entropy

In Figure 11, the fourth-order Binder's Cumulant has been plotted. As before, the curve tends to be steeper with increasing lattice size.

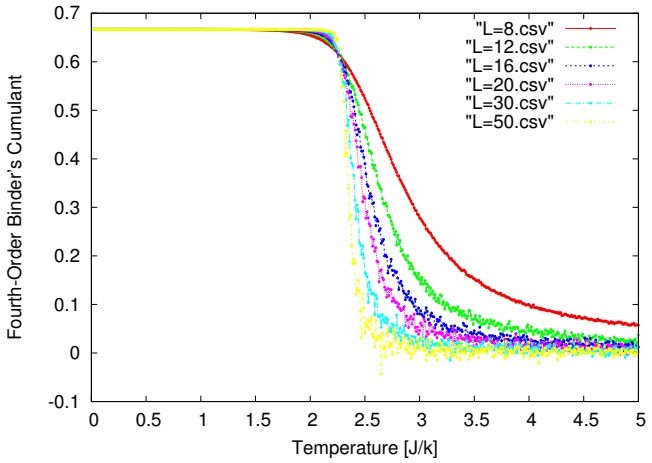

Figure 11: Fourth-Order Binder's Cumulant per spin, U_L vs Temperature, T

We find that the curves for different lattice sizes intersect at around $T = 2.26$, which marks the Critical Temperature [1]. Hence, we conclude that the Néel temperature, T_c, exists at $T = 2.26$, which is very close to the theoretical value, $k_B T_c/J = \frac{2}{ln(1+\sqrt{2})} \approx 2.26918531421$.

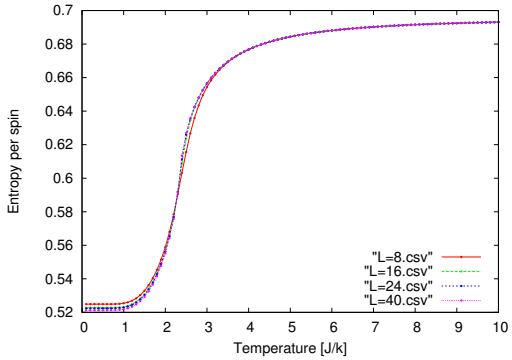

Figure 12: Entropy per spin vs Temperature, T

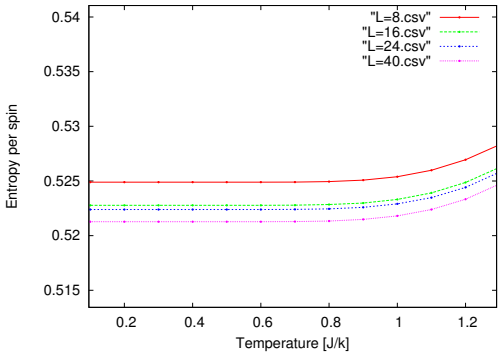

Figure 13: Downward shift in the curve with increasing lattice size

Here, in Figure 12, we have plotted the value of Entropy per spin as a function of temperature. For all the lattice sizes, the curves seem to plateau for higher temperatures to the value $ln(2) \approx 0.6931$. For lower temperatures, there seems to be a titchy downward shift in the curves (Figure 13), which was unexpected since all the curves should have converged to the same value for lower temperatures, since we are looking at the entropy per spin (which is intrinsic). Another unexpected behaviour seems to be the value to which it is converging at lower temperatures, which should have been zero, due to the system attaining an ordered phase.

5.4 Histograms for the Square Lattice

Each small square on the lattice can be assigned a number from the set $\{0, 1, 2, \ldots, 15\}$ as already shown in Figure 2. We have plotted histograms for the total number of squares in the lattice belonging to different configuration, for various temperature scales

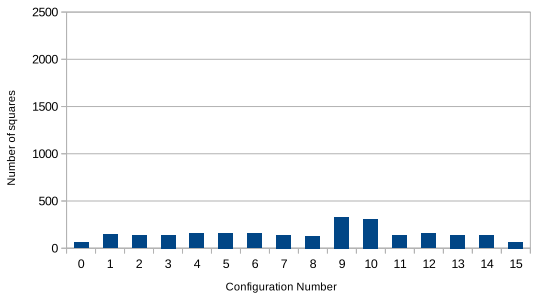

(a) $T > T_s$

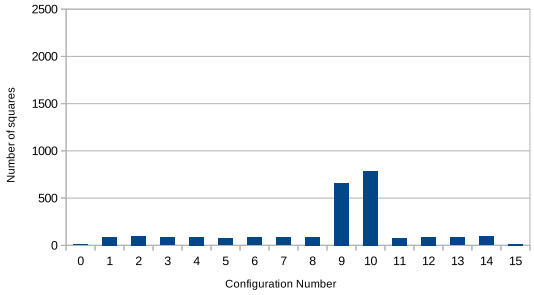

(b) $T \approx T_s$

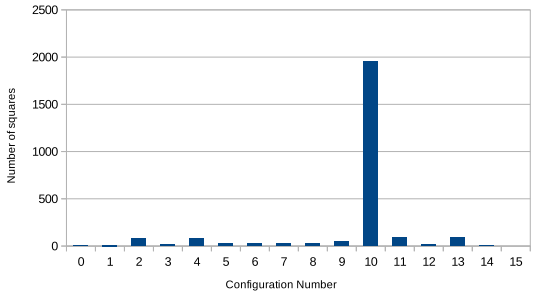

(c) $T \approx T_c$

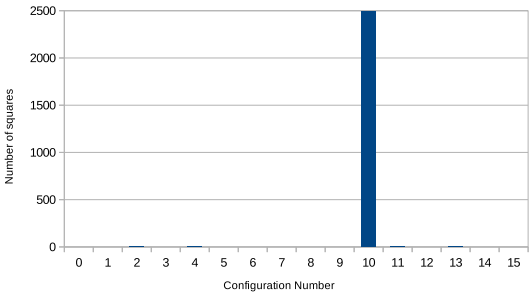

(d) $T < T_c$

Figure 14: Histograms for a square lattice of size, $L = 50$

From these figures, it is evident that at elevated temperatures, all the possible configurations exist on the lattice. Moreover, on decreasing the temperature below a certain value T_s (that will be discussed briefly in the subsequent sections), the configurations 9 and 10 start to dominate, but they remain almost equal to each other. On decreasing the temperature further below another critical level, the system randomly picks up one of configurations, either the 9^{th} or the 10^{th}. This critical level is the temperature that we have been calling the Critical Temperature, T_c so far. In this case, we find that on decreasing the temperature, we encounter the T_s first and then T_c. Later, we will vary the value of J'/J, and try to check whether there exists a crossover, i.e., whether we will ever encounter only T_s but no T_c. The temperature at which T_c and T_s coincide could be defined as the *crossover* temperature [6].

6 The Triangular Limit $(J'/J = 1)$

Due to geometrical frustration existing in the case of a triangular lattice, we expect a large number of degenerate states of the system at lower temperatures [7].

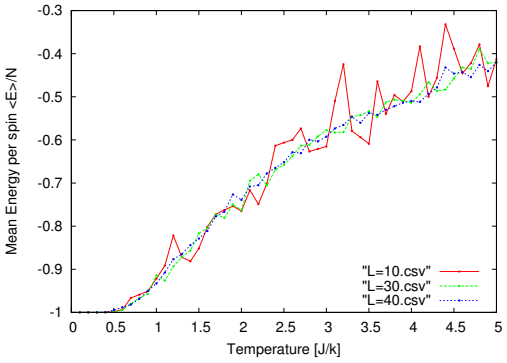

Figure 15: Entropy per spin vs Temperature, T for triangular lattices

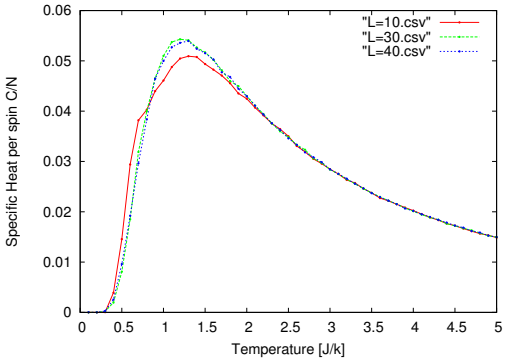

Figure 16: Specific Heat per spin, C/N vs Temperature, T for triangular lattices

There is no steep rise in the Mean Energy per spin curve, instead the energy seems to be increasing in proportion to the temperature (Figure 15). This gives an idea that there may not exist any Critical Temperature for this configuration of the lattice. The Specific Heat curve exhibits a wider maximum as compared to the square lattice case (Figure 16).

The histogram for the number of triangles with three *unhappy* bonds and that with one *unhappy* bond for every temperature has been plotted in Figure 17. We find that the number of triangles with one *unhappy* bond dominates at all temperatures, whereas the number of triangles with 3 *unhappy* bonds goes on decreasing with increase in temperature. This is in accordance with our expectation that the system will want to minimize its energy and choose to be in the state where each triangle has only one *unhappy* bond (since that is the configuration which gives minimum energy).

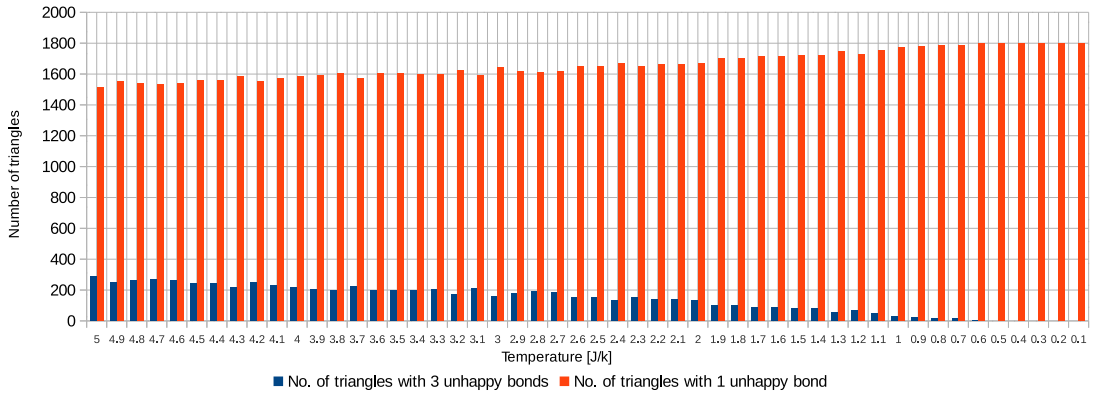

Figure 17: Histogram for a triangular lattice of size, $L = 30$

7 Interpolating between Square and Triangular Lattices

In this section, we will try to formulate the phase plot of the system and see how the Critical Temperature, T_c varies with J'/J. We expect the Critical Temperature,

to decrease with increase in J'/J value and approach zero for $J'/J = 1$, since a triangular antiferromagnetic Ising Model doesn't undergo a phase transition. We are also interested in qualitatively finding out the behaviour of T_s with respect to J'/J, and whether or not the curve of T_s vs J'/J intersect the Critical Temperature curve. From Figure 14, we know that $T_s > T_c$ for $J'/J = 0$. hence we expect that one of the following cases might occurs, viz, (a) $T_s \geq T_c$ for all $0 < J'/J < 1$ or (b) there exists a crossover temperature, T_{cross} where the curves for T_c and T_s intersect.

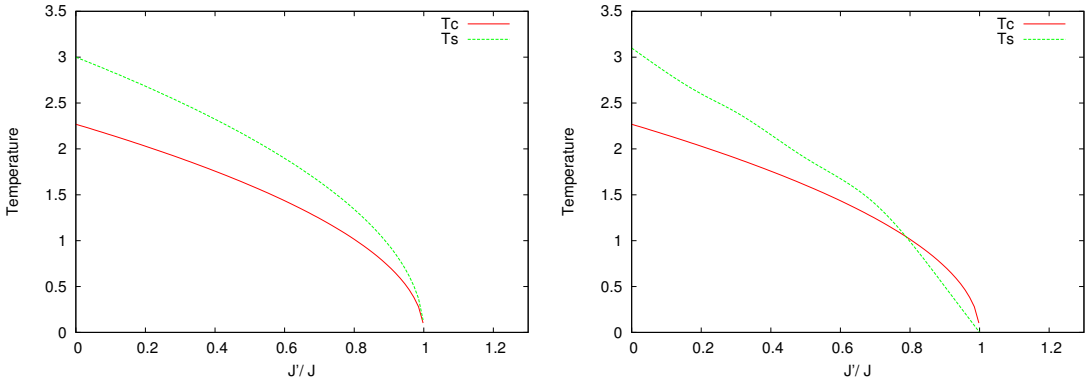

(a) $T_s \geq T_c$, no T_{cross} exists

(b) existence of a T_{cross}

Figure 18: Rough sketches estimating the phase plot of the system

7.1 Locating the Critical Temperature for different values of J'/J

For the purpose of plotting, the value of T_c has been acquired using the Binder's Cumulant plot for $0 < J'/J < 0.8$, after which the Binder's Cumulant became chaotic (since we were using the *order parameter* of the square lattice even near the triangular limit, it wouldn't give the expected results). For $J'/J > 0.8$, T_c was only qualitatively determined using the histogram of number of configurations. For values of J'/J closer to 1, there didn't exist any Critical Temperature, since no histogram at any temperature peaked for any particular configuration, though it had almost equal peaks for configurations 9 and 10. This suggests that there might actually have been a *crossover* temperature. For instance, we ran the simulation for $J'/J = 0.80$, $J'/J = 0.85$ and $J'/J = 0.90$ and plotted the histograms (Figure 21). A careful observation of these histograms leads us to infer the following details:

(i) For $J'/J = 8.00$, on decreasing the temperature sufficiently enough, we started getting the peaks for configurations 9 and 10. On further lowering the temperature, the system chose configuration 9 as the ground state. This ensures that we did hit T_s before T_c. Hence, in this case, $T_s > T_c$.

(ii) For $J'/J = 0.85$, a similar thing happened as above, except for the fact that the value of T_c was lower for $J'/J = 0.85$ as compared to that for $J'/J = 0.80$, which was expected. Also, this time, the system chose to be in configuration 10.

(iii) For $J'/J = 0.90$, we did not see any particular configuration from amongst 9 or 10 getting fixed, though at low enough temperatures ($T \approx 0.2$), we did observe two approximately equal peaks, pointing towards a possible T_s. Hence, for this case, the phase transition never occured. At such low temperatures too, the system was disordered enough to not attain any particular ground state which was expected. This also suggests that there did occur a *crossover* somewhere between $J'/J = 0.85$ and $J'/J = 0.90$. Hence, we would expect the system to behave like Figure 18 (b).

7.2 When $0.8 < J'/J < 0.9$

We tried to analyse the Specific Heat and Entropy plots for various values of J'/J between 0.8 and 0.9. For $J'/J \geq 0.85$, we observed that the Specific Heat per spin vs temperature curve peaked at two values of temperatures (Figure 19), contrary to the case with $J'/J < 0.85$, where the curve had only one peak. Similary, the Entropy per spin vs temperature curve showed two plateaus, the usual one at higher temperatures and another tiny plateau at a lower temperature, which was approximately around the same value where the specific heat curve had the second peak. The plots for Specific Heat per spin and Entropy per spin are shown below for $J'/J = 0.89$. We find that each of the specific heat curves have one sharp and narrow peak and another shorter but broader peak at a temperature higher than that of the sharp peak .

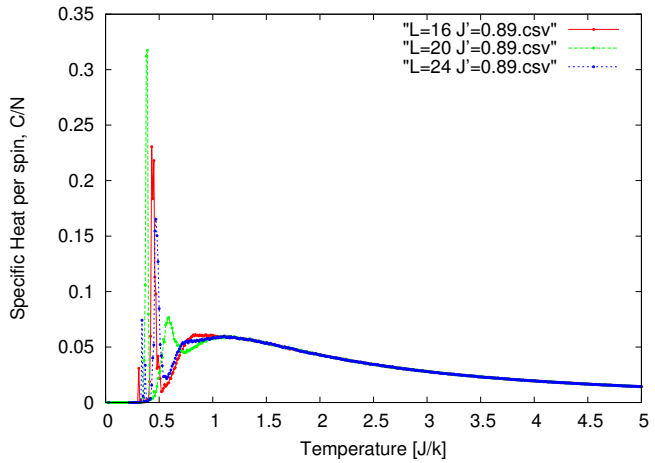

Figure 19: Specific Heat per spin vs Temperature showing two peaks for $J'/J = 0.89$ for different lattice sizes

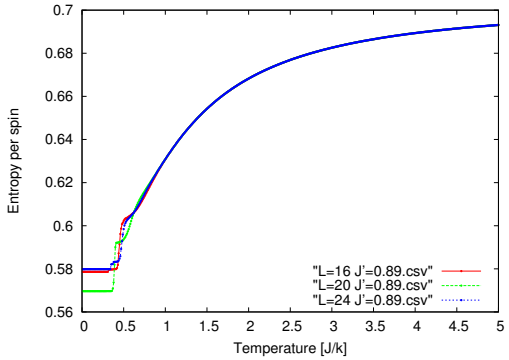

(a) Kink in the curve, showing existence of two possible plateaus

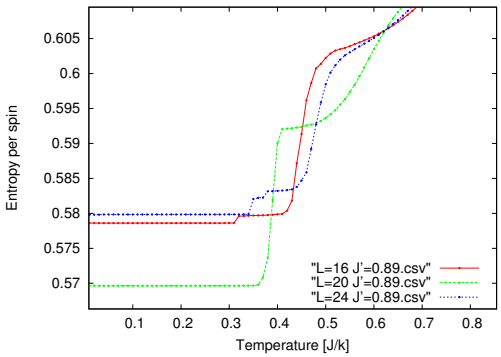

(b) Zooming near the plateau region at lower temperature

Figure 20: Entropy per spin vs Temperature for $J'/J = 0.89$

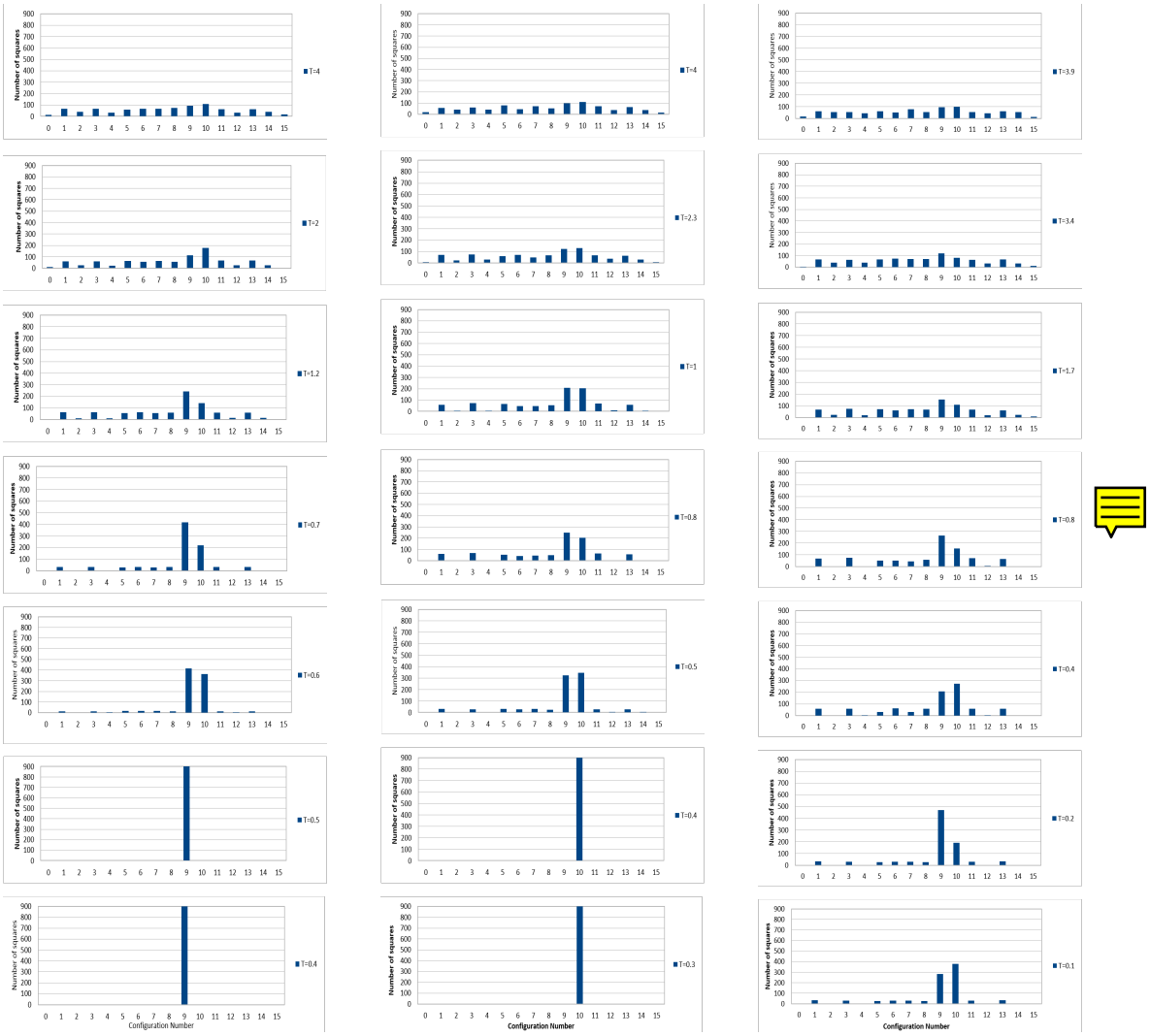

(a) $J'/J = 0.8$ (b) $J'/J = 0.85$ (c) $J'/J = 0.9$

Figure 21: Histograms for a square lattice of size, $L = 30$ for different values of J'/J (Histograms were plotted for all temperatures, only some relevant ones are shown here)

References

[1] K. Binder. Finite size scaling analysis of ising model block distribution functions. *Zeitschrift für Physik B Condensed Matter*, 43(2):119–140, 1981.

[2] Charles Kittel. *Introduction to Solid State Physics*. John Wiley & Sons, Inc., New York, 8th edition, 2005.

[3] David Landau and Kurt Binder. *A Guide to Monte Carlo Simulations in Statistical Physics*. Cambridge University Press, New York, NY, USA, 2005.

[4] David J. C. MacKay. *Information Theory, Inference & Learning Algorithms*. Cambridge University Press, New York, NY, USA, 2002.

[5] Lars Onsager. Crystal statistics. i. a two-dimensional model with an order-disorder transition. *Phys. Rev.*, 65:117–149, Feb 1944.

[6] Rico Pohle, Owen Benton, and L. D. C. Jaubert. Reentrance of disorder in the anisotropic shuriken ising model. *Phys. Rev. B*, 94:014429, Jul 2016.

[7] G. H. Wannier. Antiferromagnetism. the triangular ising net. *Phys. Rev.*, 79:357–364, Jul 1950.